

Available online at www.sciencedirect.com**ScienceDirect**

Procedia Materials Science 9 (2015) 419 – 427

Procedia
Materials Sciencewww.elsevier.com/locate/procediaInternational Congress of Science and Technology of Metallurgy and Materials, SAM –
CONAMET 2014

Fatigue life of GMAW and PAW welding joints of boron microalloyed steels

Hernán G. Svoboda^{a,b,*}, Horacio C. Nadale^a^a*GTSyCM3, INTECIN, Faculty of Engineering, University of Buenos Aires, Las Heras 2214, Buenos Aires (1127), Argentina*^b*CONICET, Rivadavia 1917, Buenos Aires, Argentina*

Abstract

Recently boron microalloyed steels have become an alternative in weight saving in structural elements in automotive industry, especially for parts like pillars and columns and reinforcements. These materials are used as quenched and tempered, reaching strength values between 1000 and 1500 MPa. Welding is a relevant issue as a fabrication process in automotive industry, in particular for high strength steels. Furthermore, fatigue life of these welded joints plays a very important role for these applications. Gas metal arc welding (GMAW) is one of the more widely used welding processes in automotive industry. Indeed, different aspects of plasma arc welding (PAW) make it an interesting option for these applications. The objective of this work was to evaluate the fatigue life of GMAW and PAW welded joints of boron microalloyed steels, in a quenched and tempered condition. Samples of 100×100 mm were butt welded by GMAW and PAW and microstructural and mechanically characterized. Fatigue curves were obtained for both processes in a four point bending configuration. It was observed that PAW welded samples had a higher fatigue life than those welded by GMAW. Weld bead toes of GMAW joints acted as geometric stress concentrators, being the main responsible for fatigue resistance reduction.

© 2015 The Authors. Published by Elsevier Ltd. This is an open access article under the CC BY-NC-ND license (<http://creativecommons.org/licenses/by-nc-nd/4.0/>).

Peer-review under responsibility of the Scientific Committee of SAM–CONAMET 2014

Keywords: Boron microalloyed steels; GMAW; PAW; microstructure; fatigue

* Corresponding author. Tel.: +054-11-4514-3009; fax: +054-11-4514-3013

E-mail address: hsvobod@fi.uba.ar

1. Introduction

Boron microalloyed steels (BMAS) are part of advanced high strength steels and in the last years have become in an alternative for weight reduction of structural parts in automotive industry. Particularly with the development of hot stamping process these steels have reach a special impulse for its use in parts with complex geometries like columns, reinforcements, pillars, etc. These materials are hot forged and then quenched and tempered, achieving tensile strengths between 1000-1500 MPa and reducing significantly the springback [World Steel Association (2014), Dilthey and Ste (2005)].

Nomenclature

AHSS	Advance High Strength Steels
b	Basquin exponent
BM	Base Metal
BMAS	Boron Microalloyed Steels
FI	Fatigue Index
GMAW	Gas Metal Arc Welding
HAZ	Heat Affected Zone
CG-HAZ	Coarse-grained HAZ
FG-HAZ	Fine-grained HAZ
HI	Heat input
HV	Vickers microhardness
HV _{min}	Minimum Vickers microhardness
IC	Inter-critical HAZ
I _f	Fatigue Index
I _H	Hardness Index
I _σ	Strength Index
K _t	Stress concentration factor of weld toe
LM	Light Microscopy
MHZ	Minimum hardness zone
N _f	Cycles to Failure
PAW	Plasma Arc Welding
Q+T	Quenching and Tempering
θ	Weld toe angle
R	Fatigue Stress Ratio
ρ	Weld toe radius
SEM	Scanning Electron Microscopy
SC	Sub-critical HAZ
σ _a	Stress amplitude
σ _f	Fatigue limit
σ' _f	Basquin coefficient
σ _{uts}	Ultimate Tensiles Stress
WM	Weld Metal

Welding of these materials is a relevant aspect for automotive industry. Among welding processes employed in this industry, GMAW is one of the more used, as well as RSW, LW and PAW [World Steel Association (2014)]. For AHSS, the joint efficiency decrease with the increase in the material strength, due to the formation of softened zones in the HAZ [World Steel Association (2014); Farabi et al. (2010)]. The fatigue life of these welded joints is also a very important issue [World Steel Association (2014)]. Geometric aspects as the stress concentration produced by the weld toe or other welding defects, residual stresses and microstructural features will define the

fatigue life of the welded joints [Radaj (1996)]. In this context the information available about the fatigue life of welded joints involving BMAS is scarce, as well as the effect of the welding process and its parameters.

The objective of this work was to study the fatigue life of welded joints of BMAS in Q+T condition, produced by GMAW and PAW.

2. Experimental procedure

To reach the proposed objectives a sheet of BMAS with a thickness of 1 mm was used. Chemical composition was determined and heat treatment of quenching and tempering was done on samples of 50×100 mm. It consisted in austenization to 875 °C during 10 min followed by quenching in oil, then tempering at 475 °C during 30 min. The obtained material in Q+T condition was characterized microstructurally and mechanically by LM, SEM, Vickers microhardness and tensile test.

Q+T samples were butt welded by GMAW and PAW in mechanized form. Fig. 1 shows the experimental set up for both welding processes. In Table 1, the welding parameters used for both welding processes are presented.

Table 1. Welding parameters.

Proc.	I (A)	V (V)	V (mm/seg)	Gas	Q (L/min)	HI (J/mm)
GMAW	85	19	15.6	Ar-20CO ₂	20	0.11
PAW	50	13.5	7.7	Ar/Ar-5H ₂	0.8/20	0.09

For GMAW process the filler metal was a solid wire ER70S6 of 0.8 mm in diameter. The torch angle was 15° pushing, the contact tip-work piece distance was 13 mm and it was used a backing plate of 5 mm thick of aluminum. For PAW process the torch angle was 10° pushing, the retreating of the electrode was 1 mm, and the tip-work piece distance was 2 mm.

It can be seen that the electric parameters are slightly lower in PAW than in GMAW, but it was compensated with welding velocity, looking for a similar heat input (HI) in both processes.

The welded samples obtained by both processes were microstructurally and mechanically characterized by means of LM, SEM, HV and transversal tensile test.

Indeed, for both processes fatigue tests in four point bending, with the face of the samples in tension were done, using a stress ratio $R=0.1$ and a test frequency of 20 Hz, to obtain the fatigue curve σ_a-N . The span used was 80 mm and 40 mm for the upper actuator. Fig. 2(a) shows a scheme for test probes extraction for fatigue and tensile tests.

On every GMAW fatigue test sample, previously to the fatigue testing, the geometric aspects related to the weld toe, according to Fig. 2(b). From the radius and angle the K_t factor was calculated using the methodology proposed by Lagoda (2008). On each sample the four toes were analyzed, obtaining finally an average value for K_t .

After fatigue testing, some of the testing samples were characterized using LM and SEM.

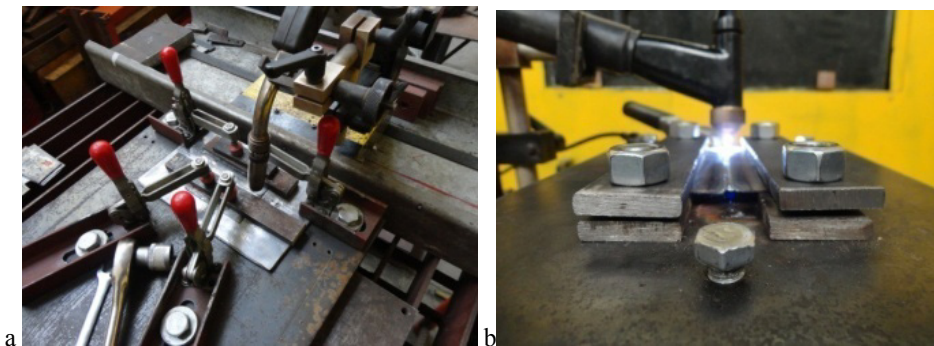


Fig. 1. Experimental set-up: (a) GMAW; (b) PAW.

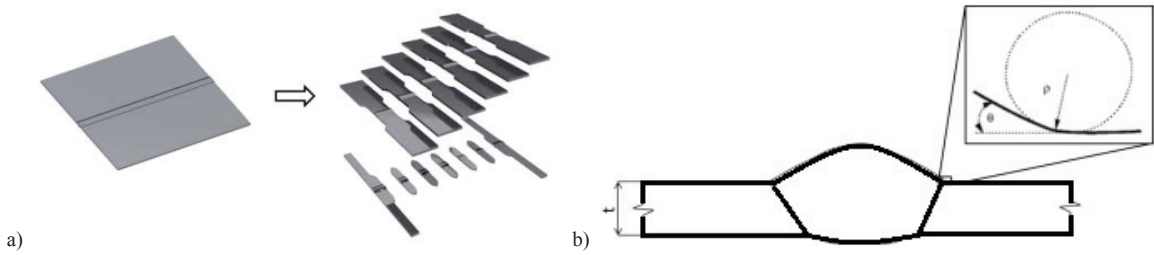


Fig. 2. (a) Samples extraction for tensile and fatigue testing of welded joints; (b) geometrical aspects measurements in GMAW weld toe.

3. Results and discussions

In Table 2 the chemical composition of the analyzed material is shown.

Table 2. Chemical composition (wt%).

C	Mn	Si	P	S	B	Fe
0.28	1.17	0.16	0.016	0.012	0.0031	Bal.

It can be seen that the material corresponds to medium carbon steel, with Mn and 30 ppm of B. In Fig. 3, the microstructure obtained after the Q+T heat treatment is shown.

The obtained microstructure consisted in a uniform tempered martensite, with a Vickers microhardness of 300 +/-8 HV. The 0.2% proof stress was 877 MPa and the ultimate tensile strength was 940 MPa, with a specific elongation to fracture of 5%, obtained in longitudinal samples respect to the rolling direction.

In Fig. 4, images of the welded joints obtained for both processes are shown.

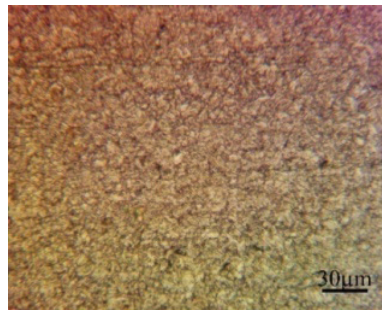


Fig. 3. Microstructure of base material in Q+T condition.

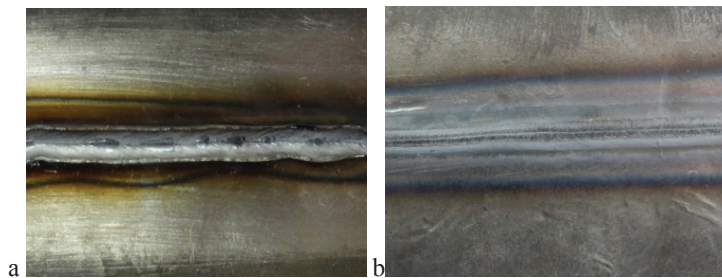


Fig. 4. Surface aspect of welded samples: (a) GMAW; (b) PAW.

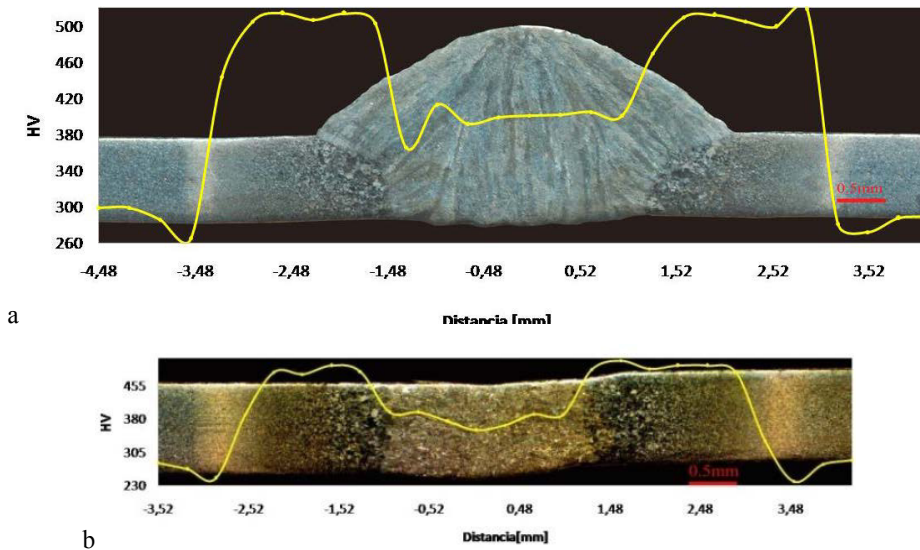


Fig. 5. Macrographs and Vickers microhardness profiles: (a) GMAW; (b) PAW.

GMAW presents the typical reinforcement of welding process with filler material while PAW does not have it, due to its autogenous condition. Indeed a good surface aspect and the absence of defects can be seen.

Macrographs and microhardness profiles of both welded joints are shown in Fig. 5.

In Fig. 5(a), in the macrograph of GMAW joint, the different zones produced by the welding thermal cycle are observed: the weld metal (WM), the heat affected zone (HAZ) and the base metal (BM). Also, it can be seen the absence of internal defects like porosity or cracking, showing a very good root conformation with complete penetration. Indeed the wetting of WM on BM in the weld toes can be observed, which represent a stress raisers that will affect the fatigue life of the welded joint [Radaj (1996)].

Vickers microhardness profiles show a slightly decrease from the BM hardness (300 HV) to the weld centerline, reaching a minimum at the subcritical/intercritical zone of 266 HV. This could be associated to the tempering of the martensite. Then the microhardness values increase up to reach 500 HV near the fusion line, into the HAZ. This fact is related with the partial or total austenization reaching that will form fresh martensite during cooling. Finally in the WM the microhardness decrease up to 380 HV, due to the dilution of the BM with the filler metal.

For PAW welded joint [Fig. 5(b)] there are also no internal defects, a good root conformation and full penetration, without undercut or reinforcement. In this sense, this process does not present stress raisers related with geometric aspects.

The evolution of microhardness along the welded joint, shows a profile very similar to that obtained for GMAW welded joint, with $HV_{min}=239$ HV and peak values and WM values very similar. Indeed, HAZ and WM sizes are also very similar to the GMAW ones. This could be related with the similar HI applied in both cases.

Figs. 6(a) and (b) show the microstructural evolution for both GMAW and PAW welded joints, respectively.

In both cases a very similar microstructural evolution is observed. From BM up to WM it passes thru different zones which constitute the HAZ. Adjacent to the BM is the subcritical zone (SC) where the martensite is submitted to a high temperature tempering. Then it is the intercritical zone (IC) where the partial austenization allows the formation of a fraction of fresh martensite. Next to IC zone there is the fine grain HAZ (FG-HAZ) and the coarse grained HAZ (CG-HAZ) where complete austenization takes place and grain size increase with the proximity to the fusion line. This last zone corresponds to the maximum hardness value. In the WM due to the dilution of the BM with the filler metal the hardness is lower and no martensitic structures (bainite) could be form. These observations are consistent with the microhardness profiles of Fig. 5.

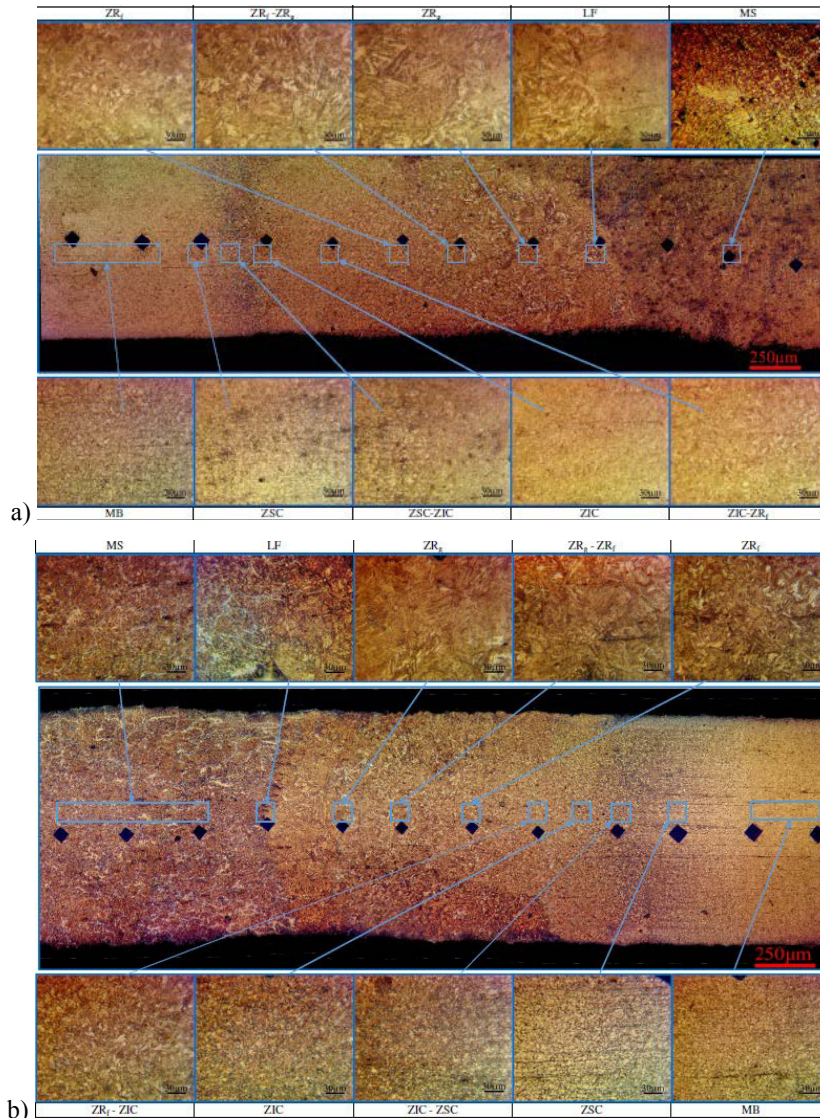


Fig. 6. Microstructural evolution in the several zones of the welds: (a) GMAW; (b) PAW.

In Table 3, the mechanical properties of both welded joints are presented, as well as joint efficiency and hardness index $I_H = H_{BM}/HV_{min}$

Table 3. Mechanical properties of welded joints.

Proc.	HV _{min}	σ _{uts} (MPa)	I _H	I _σ
GMAW	266	912	0.89	0.97
PAW	239	915	0.80	0.97

The joint efficiency for both processes was high, reaching 97%. The I_H was something lower, especially for PAW. The fracture was located at MHZ, for both cases. In Table 4, the geometric aspects results of the GMAW fatigue samples are presented, as well as the average calculated value of K_t and K_{tmax}.

Table 4. K_t values measured on GMAW fatigue test samples.

Proc.	ρ (mm)	θ (°)	$K_{t\text{prom}}$	$K_{t\text{max}}$
GMAW	0.61	40	1.17	1.21

The values of ρ and θ are the average of four measures on ten samples. $K_{t\text{max}}$ was determined as the average of the $K_{t\text{max}}$ of each sample. It can be seen that the local stress is 20% higher for samples welded with GMAW, due to the effect of the stress raiser of the weld toe.

In Fig. 7, the fatigue curves obtained for both welding processes are shown.

PAW welded joints presents a higher fatigue strength than GMAW ones with more difference in high cycle regime. This fact could be explained by the stress concentration produced in the weld toe of the GMAW joints, which magnify locally the stress value, requiring a lower number of cycles to produce the fatigue failure than PAW ones. This effect is amplified at lower stress level [Xu et al. (2013)].

Basquin constants were obtained from the correlation with the experimental data. In Table 5, the fatigue limit, Basquin constants values and the fatigue index ($I_f = \sigma_f / \sigma_{\text{uts}}$) obtained for both GMAW and PAW are presented. The fatigue limit was defined as the fatigue strength for 10^7 cycles.

Table 5. Fatigue limits and Basquin constants for both welding processes.

Proc.	σ_f (MPa)	σ_{uts} (MPa)	I_f	σ'_f (MPa)	b
GMAW	150	912	0.16	624	-0.13
PAW	250	915	0.27	1345	-0.05

Fatigue index for GMAW welded joints was lower than for PAW ones, which reaches 0.27. This value is higher than those obtained previously for welded joints of AHSS [Xu et al. (2013), Bonello and Svoboda (2013)]. The Basquin constants are values of technological interest to estimate fatigue life of welded structures with these materials and processes.

For GMAW fatigue tested samples in all cases the cracks nucleated at the weld toe, as was expected [Figs. 8(a)-(c)].

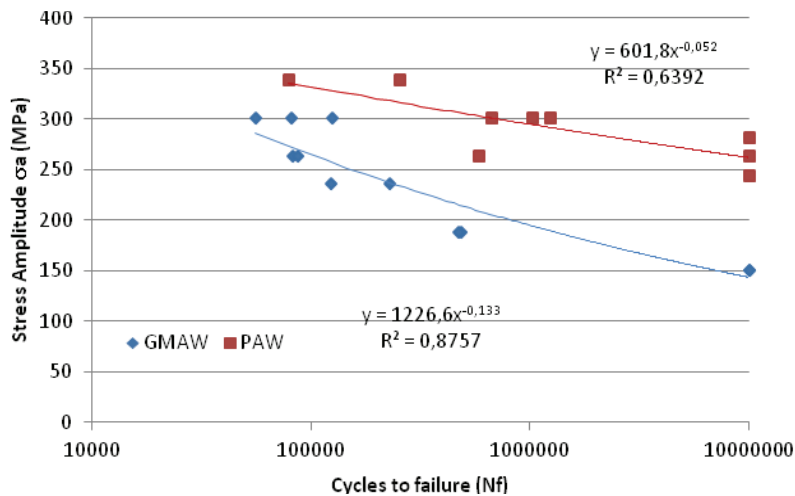


Fig. 7. Fatigue curves for GMAW and PAW welded joints.



Fig. 8. Fracture location for GMAW fatigue tested samples.



Fig. 9. Fracture location for PAW fatigue testing samples: (a) MS; (b) MB; (c) ZRG.

In Fig. 8(b), it can be observed that the fissure nucleates at the weld toe and propagates in a direction orthogonal to the tensile stresses. In Fig. 8(c), a detail of the nucleation site can be observed, locating where the fusion line reach the free surface, and then the propagation proceeds thru CG-HAZ and FG-HAZ at the bottom.

For PAW welded joints, the crack nucleates in different zones, depending on the stress level. For high stress level the fracture was located into the WM in the central shrinkage or in the fusion line [Fig. 9(a)]. For medium stresses it was at MHZ or in BM [Fig. 9(b)], and for lower stress levels the nucleation site was positioned in the CG-HAZ [Fig. 9(c)]. These observations has been previously reported for steels of lower strength [Xu et al. (2013)] and they can be associated to the absence of severe geometric stress raisers, which allows that metallurgical aspects became relevant.

In Fig. 10, fracture surface SEM images of a GMAW sample are shown.

In Fig. 10(a) the initiation zone is shown whereas in Fig. 10(b) striations of propagating zone can be seen. Secondary cracks are also observed. These aspects are consistent with the previously observed for this type or welded joints [Xu et al. (2013)]. There were no significant differences in the fracture surfaces for different welding processes.

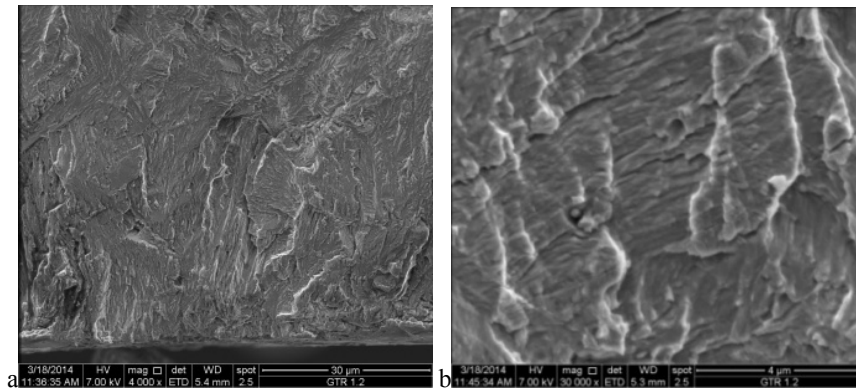


Fig. 10. Fracture surfaces for fatigue tested samples: (a) initiation zone, (b) propagation zone.

4. Conclusion

In the present work butt welded joints of BMAS of 1 mm thick in Q+T condition, obtained by GMAW and PAW processes were microstructural and mechanically analyzed. Tensile and fatigue behavior were evaluated.

The procedures for both welding processes were successfully applied producing defects free welded joints.

Both obtained joints presented inside the HAZ a softened zone (240-270 HV) with respect to the base material (300 HV) associated to the tempering of the martensite, as well as a hardened zone (500HV) near the fusion zone, associated to the formation of fresh martensite. In the WM the microhardness was something lower reaching 360-400 HV, due to dilution of the base metal with the filler material. In tensile test, both processes achieve high joint efficiencies of 97%, being the location of the fracture in the MHZ in the HAZ.

Fatigue life of PAW welded joints was significantly higher than the GMAW ones, with a fatigue limit 78% higher. This could be associated to the local stress magnification at the toe of GMAW beads. In this process the cracks nucleated at the mentioned weld toe. For PAW fatigue samples the fracture was located at WM for high stresses, at BM or MHZ for medium stresses and at HAZ-CG for lower applied stresses.

Acknowledgements

Authors are grateful to INTI-Mecánica for chemical analysis and SEM, Ternium Siderar for material provision and to Ing. Horacio De Rosa. This Project is partially supported by University of Buenos Aires and ANPCYT.

References

- Bonello, T., Svoboda, H., 2013, Efecto del modo de transferencia en el proceso GMAW sobre la vida a la fatiga de uniones soldadas de aceros DP750, XI Congreso Regional de Ensayos No Destructivos y Estructurales, Mar del Plata, Argentina.
- Dilthey, U., Ste, L., 2005, Multimaterial car body design: challenge for welding and joining., *Science and Technology of Welding and Joining* 11(2), 135-142.
- Farabi, N., Chen, D., Shou, Y., 2010, Fatigue properties of laser welded dual-phase steel joints, *Procedia Engineering* 2(1), 835-843.
- Lagoda, T., 2008, *Lifetime estimation of welded joints*, Springer, Berlin.
- Radaj, D., 1996, Review of fatigue strength assessment of nonwelded and welded structures based on local parameters, *International Journal of Fatigue* 18, 153-170.
- World Steel Association, Committee of Automotive Applications, *Advanced High Strength Steels (AHSS): Application Guidelines (5.0 Version)*. Brussels: World Steel Association, 2014.
- Xu, W., Westerbaan, D., Nayak, S., Chen, D., Goodwin, F., Zhou, Y., 2013, Tensile and fatigue properties of fiber laser welded high strength low alloy and DP980 dual-phase steel joints, *Materials and Design* 43, 373-383.